



resulting values are  $a=7.1154\text{\AA}$  and  $c=19.4293\text{\AA}$ , which are consistent with the standard values (JCPDS40-1407). The crystallite size, dislocation density and strain were calculated by considering high intense diffraction peaks of the deposited films using the following equations and the values are tabulated in Table 1.

$$D = K\lambda / \beta \cos\theta \quad (1)$$

where  $K$  is the shape factor,  $\theta$  is the Bragg's angle,  $\lambda$  is the wavelength of X-rays used and  $\beta$  is the width of the peak at the half of the maximum peak intensity. The dislocation density ( $\delta$ ) was determined using Williamson and Smallman's formula [9]. The dislocation density was calculated from the crystallite size of the deposited samples. The increase in crystallite size is due to the aggregation or coalescence of small nanocrystalline particles.

$$\delta = 1/D^2 \quad (2)$$

The line broadening gets reduced because of increase in crystallite size and decrease in strain of the material. The strain ( $\epsilon$ ) is obtained using the relation

$$\epsilon = (\beta \cos\theta)/4 \quad (3)$$

In order to induce photoactivity the films were post heat treated at different temperatures in argon atmosphere for 20 min in the temperature range of 450 - 550°C. Fig.2 show the XRD pattern of the films deposited at 50 % duty cycle and post heated at different temperatures. It is observed that the peaks become sharp due to recrystallization. The microstructural parameters of the post heat treated films are shown in Table.2. The crystallite size of the  $\text{In}_2\text{Se}_3$  films increases from 30 nm to 60 nm with increase of duty cycle (Table.1) and also with heat treatment temperature.

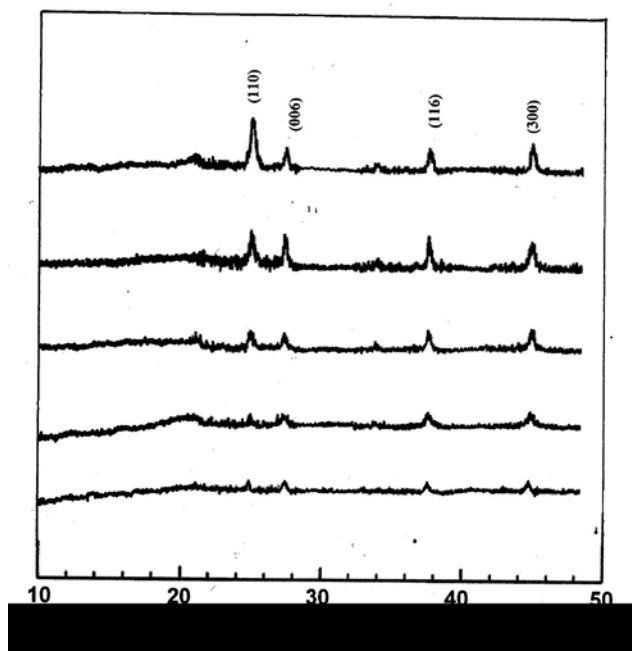


Figure 1: X-ray diffraction pattern of  $\gamma - \text{In}_2\text{Se}_3$  films deposited at different duty cycles (Top most) 50 % (Bottom most) 6 %. Duty cycle increases from bottom to top

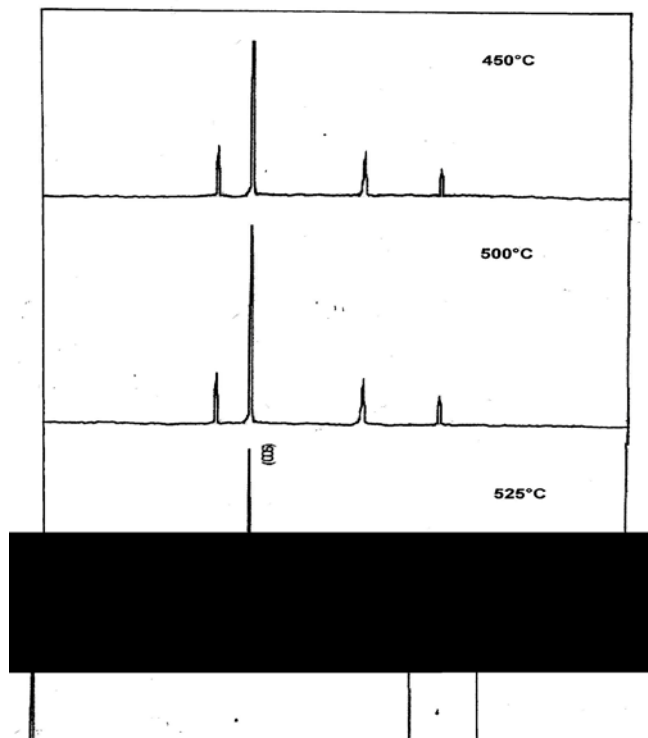


Figure 2: X-ray diffraction patterns of  $\gamma - \text{In}_2\text{Se}_3$  films post annealed at different temperatures in argon atmosphere.

Table 1: Structural parameters of  $\text{In}_2\text{Se}_3$  films deposited at different duty cycles

| Duty cycle (%) | Lattice parameters a (Å) | Lattice parameters c (Å) | Cryst Size (nm) | strain ( $\times 10^{-2}$ ) | disloc density lines $\text{m}^{-1} \times 10^{15}$ |
|----------------|--------------------------|--------------------------|-----------------|-----------------------------|---|
| 6              | 7.11                     | 19.42                    | 15              | 2.80                        | 4.44  |
| 9              | 7.12                     | 19.41                    | 20              | 2.76                        | 2.50  |
| 15             | 7.13                     | 19.43                    | 28              | 2.69                        | 1.27  |
| 33             | 7.13                     | 19.43                    | 34              | 2.60                        | 0.87  |
| 50             | 7.12                     | 19.41                    | 40              | 2.48                        | 0.63  |

Table 2: Structural parameters of  $\text{In}_2\text{Se}_3$  films deposited at 50 % duty cycle and post heat treated at different temperatures

| Heat treatment Temp (°C) | Cryst size (nm) | dislocation density lines $\text{m}^{-1} \times 10^{14}$ | strain ( $\times 10^{-2}$ ) |
|--------------------------|-----------------|--|-----------------------------|
| 450                      | 80              | 1.56   | 1.58                        |
| 500                      | 100             | 1.00   | 1.42                        |
| 525                      | 115             | 0.76   | 1.29                        |

Composition of the films was studied by EDS analysis. The atomic ratio of approximately 2 :3 was observed in all cases. For the films deposited at lower duty cycles, there was a slight excess of Selenium. The atomic concentration was In – 38.50 %, Se – 41.50 % at 6 % duty cycle, with increase of duty cycle, the atomic concentration was In – 39.90 % and Se – 40.10 % at 50 % duty cycle. Fig.3 shows the EDS spectrum of  $\text{In}_2\text{Se}_3$  films deposited at 50 % duty cycle.

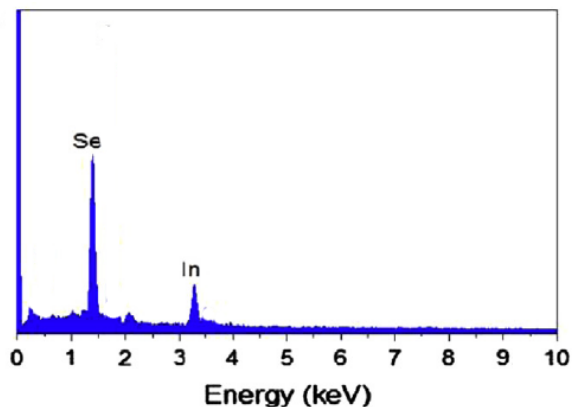


**Figure 3:** EDS spectrum of  $\text{In}_2\text{Se}_3$  film deposited at 50 % duty cycle

Surface morphology of the films deposited at different duty cycles was studied by Atomic force microscope. Fig.4 shows the atomic force micrographs of the films.

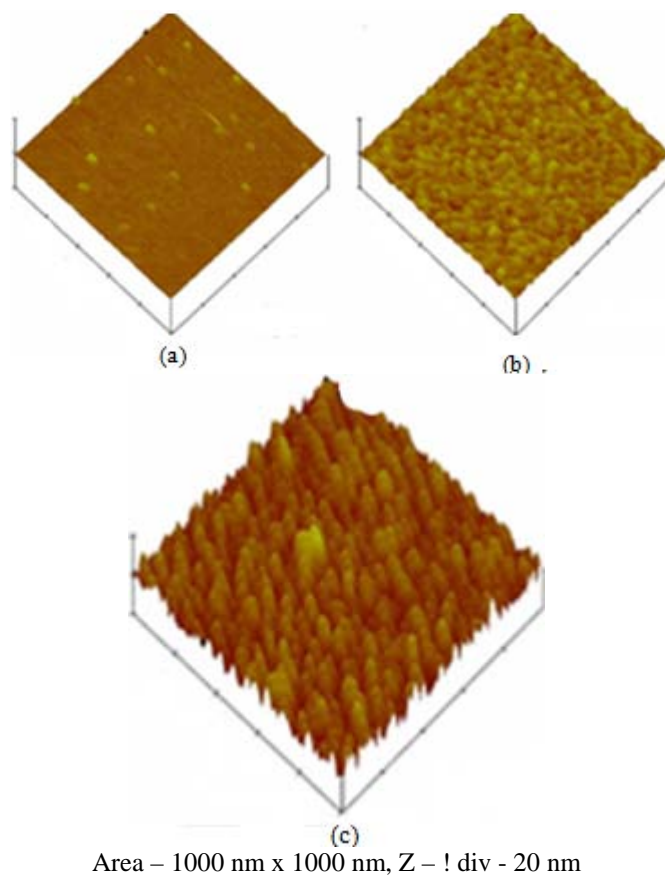


**Figure 4:** AFM of  $\text{In}_2\text{Se}_3$  films deposited at different duty cycles (a) 9 % (b) 33 % (c) 50 %

For measuring the photoconducting properties, the surface of the films were vacuum evaporated with Indium contact on the edges of the film. It is observed that the films deposited at 50 % duty cycle exhibited the maximum photosensitivity; hence further studies were carried out on these films. Fig.5 shows the variation of photosensitivity (PS) with intensity of illumination for the films prepared at different duty cycles.

It was observed from the figure, as the intensity of illumination increases, the corresponding photosensitivity

also increases. Of all the annealing temperatures, the cells prepared with films annealed at  $550^\circ\text{C}$  exhibited maximum photosensitivity. The dependence of PS on light intensity at room temperature can be described in terms of the oxygen absorption effects at high annealing temperatures. The thermal release of oxygen from the surface is the possible mechanism, which is always dominant for cells annealed in Argon and hence both the dark and photoconductivity are increased.

Fig.6 shows the variation in the photocurrent with illumination for the films deposited at different duty cycles. The high photosensitivity arises due to the presence of compensated acceptors, which act as sensitizing centers. As the excitation intensity is increased, these centers become more active and the photosensitivity sharply increases at some region of excitation. It is observed from the figure, that upto 5000 lux, the photocurrent varies linearly with illumination, becoming super linear above this intensity. The super linearity arises from the conversion of hole traps into recombination centers when the hole quasi Fermi level moves towards the valence band with an increase in light intensity. These recombination centers, which have higher capture cross sections for the holes than electrons, in conjunction with another set of recombination centers with equal capture cross sections for both the carriers, decrease the lifetime of the holes thereby increasing the lifetime of the electrons. While the hole traps are being converted into recombination centers, the electron lifetime is continuously increasing and the photocurrent varies super linearly with increasing light intensity [14]. The transition from linearity to super linearity occurs when the hole demarcation level is at the level of the recombination centers with equal capture cross section.

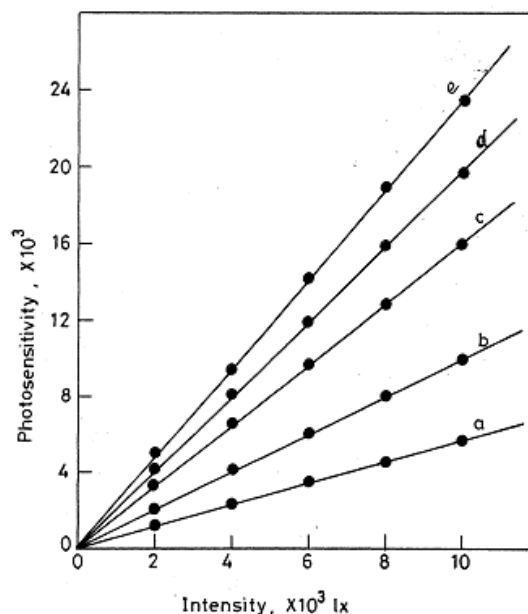


**Figure 5:** Variation of photosensitivity with illumination for the films deposited at different duty cycles (a) 6 % (b) 9 % (c) 15 % (d) 33 % (e) 50 %

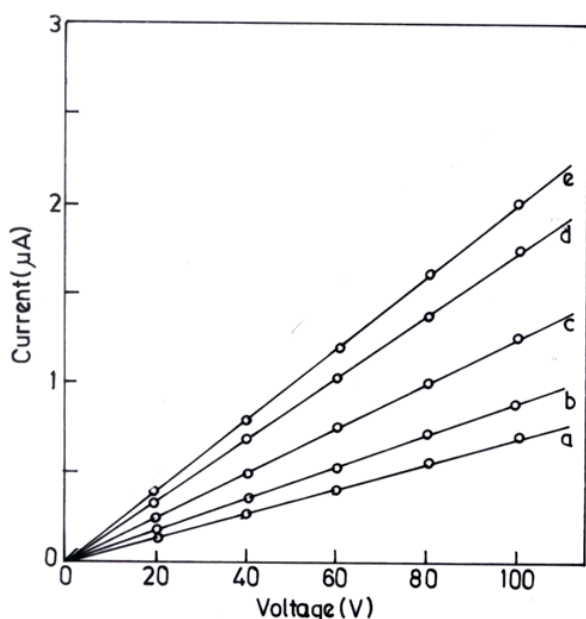


**Figure 6:** Variation of photocurrent with voltage for the films deposited at different duty cycles

#### 4. Conclusion

Nanocrystalline films with crystallite size in the range of 15 nm – 40 nm can be obtained. Single phase  $\text{In}_2\text{Se}_3$  films were prepared by the pulse electrodeposition technique. The films exhibit photoconductivity.

#### References

- [1] Hariskos D, Spiering S, Powalla M. *Thin Solid Films*, 480 (2005) 99.
- [2] Gordillo G, Calderón C. *Solar Energy Materials and Solar Cells* 2003;77(2003)163.
- [3] Pathan H, Kulkarni S, Mane R, Lokhande C. *Materials Chemistry and Physics* 93(2005)16.
- [4] Massaccesi S, Sanchez S, Vedel J. *Journal of Electroanalytical Chemistry* 412(1996)95.
- [5] Mutlu IH, Zarbaliyev MZ, Aslan F *Journal of Sol-gel Science and Technology* 43(2007)223.
- [6] Marsillac S, Combout Marie AM, Bernede JC, Conan A. *Thin Solid Films* 288(1996)14
- [7] Okamoto T, Yamada A, Konagai M. *Journal of Crystal Growth* 175 (1997)1045.
- [8] Chang KJ, Lahn SM, Chang JY. *Applied Physics Letters* 89 (2006) 18 pages.
- [9] G.B. Williamson, R.C. Smallman, *Philosophical Magazine* 1 (1956) 34.
- [10] M. Ghaemi, L. Binder, *J. Power Sources* 111 (2002) 248 - 254.
- [11] A.Marlot, P. Kern, D. Landolt, *Electrochim. Acta* 48 (2002) 29 – 36
- [12] M.E.Bahrololoom, R.Sani, *Surf.Coat.Technol*, 192 (2005) 154 – 163
- [13] K.M.Yan, *Surf.Coat.Technol*, 88(1996) 162 – 164
- [14] R.H.Bube and L.A.Barton, *J.Chem.Phys*, 29(1958) 128